THE ASTROPHYSICAL JOURNAL, 211:189–197, 1977 January 1

DOES THE UPPER MAIN SEQUENCE EXTEND ACROSS THE WHOLE H-R DIAGRAM?

RICHARD STOTHERS AND CHAO-WEN CHIN
Institute for Space Studies, Goddard Space Flight Center, NASA, New York
Received 1976 April 26

ABSTRACT

The effect of using Carson's new radiative opacities in evolutionary sequences of stellar models has been studied over the mass range 7–60 $M_\odot$. The new opacities are very large in the outer part of the envelope, and induce such enormous radii for masses greater than $\sim 30\ M_\odot$ ($Z_e = 0.02$) or $\sim 20\ M_\odot$ ($Z_e = 0.04$) that the evolutionary tracks during the phase of core hydrogen burning extend across the whole H-R diagram. The choice of the Schwarzschild or Ledoux criterion for convection makes very little difference for the behavior of the tracks. Evolution through the effective-temperature range $\log T_e = 3.6$–4.0 occurs in all cases on a rapid (secular) time scale. Core helium burning takes place exclusively in the red-supergiant configuration for stellar masses $> 8\ M_\odot$ ($Z_e = 0.02$) or $> 6\ M_\odot$ ($Z_e = 0.04$). The new stellar models seem to be in significantly better agreement with the observed distribution of bright stars on the H-R diagram than are the older models based on the Cox-Stewart opacities. It can be inferred that a large envelope opacity (e.g., Carson's) exists and that substantial mass loss takes place in very massive late-type supergiants.

Subject headings: stars: evolution — stars: interiors — stars: massive — stars: supergiants

I. INTRODUCTION

Radiative opacities are known to play an important role in determining where models of massive stars lie on the H-R diagram. For example, if atomic absorption is added to the purely electron-scattering opacity that was commonly adopted before 1968, the effective temperatures of stellar models at all stages of evolution can be markedly reduced. Very recently, Carson's (1976) new radiative opacities have led to a further reduction of effective temperatures in the case of main-sequence stars more massive than $\sim 7\ M_\odot$ (Stothers 1974*a*, 1976).

The present paper is devoted to: (1) a complete calculation of the phase of hydrogen burning in the core for massive stellar models constructed with Carson's new opacities; (2) extension of the calculations to cover the later phases of evolution up to the exhaustion of helium at the center; and (3) comparison of the resulting evolutionary tracks with observations of supergiants on the H-R diagram. Since we have already shown that stellar models constructed with the Cox-Stewart opacities cannot adequately represent real supergiants (Stothers and Chin 1975, Paper III; 1976, Paper IV), it is of considerable interest to see whether Carson's opacities can improve the situation.

II. THEORETICAL EVOLUTIONARY TRACKS

Evolutionary sequences have been computed for stars in the mass range 7–60 $M_\odot$ by using the same input physics as in our earlier work, with the exception of (1) Carson's new opacities for temperatures higher than $\log T = 3.85$ (the new low-temperature opacities are not yet completed) and (2) a convective mixing length equal to a constant multiple, α_P, of the local *pressure* scale height (a constant multiple of the local density scale height was used before). Semiconvection has been included, in accordance with either the Schwarzschild (S) or the Ledoux (L) criterion, as described in Papers III and IV. Notation used in the present paper follows our earlier papers. Here we discuss only the changes induced in the stellar models by making the change from Cox-Stewart to Carson opacities, i.e., from opacities based on a "hydrogenic" model of the atom to opacities based on the "Thomas-Fermi" model, in the case of elements heavier than hydrogen and helium.

a) Core Hydrogen Burning

Various stellar models covering the phase of core hydrogen burning are summarized in Table 1, where the following stages are represented: (*a*) zero-age main-sequence stage (ZAMS),[1] (*b*) stage where $X_c \approx 0.4$, (*c*) stage where $X_c \approx 0.2$, (*d*) stage at which overall stellar contraction begins, and (*e*) stage at which rapid envelope expansion begins. At the highest stellar masses, stage *e* occurs before stage *d* and in some cases even before stage *c*; the latter stages are not tabulated in such cases. The structural evolution of the stellar interior for masses of 15 and 30 $M_\odot$

[1] Slight differences that exist between these models and earlier ones published with the same opacities are due to a minor difference in the adopted nuclear reaction rate.

TABLE 1

SELECTED EVOLUTIONARY MODELS DURING CORE HYDROGEN BURNING

$M/M_\odot$	Criterion for Convection	Z_e	α_P	Model 1 X_c	Model 1 $\log (L/L_\odot)$	Model 1 $\log T_e$	Model 1 $\tau(10^6$ yr)	Model 2 X_c	Model 2 $\log (L/L_\odot)$	Model 2 $\log T_e$	Model 2 $\tau(10^6$ yr)
7	S or L	0.02	any	0.730	3.199	4.309	0.00	0.412	3.345	4.278	27.35
7	S or L	0.04	any	0.710	3.153	4.274	0.00	0.417	3.281	4.247	28.94
10	S or L	0.02	any	0.730	3.709	4.385	0.00	0.411	3.873	4.351	14.28
10	S or L	0.04	any	0.710	3.683	4.353	0.00	0.413	3.835	4.319	14.64
15	S	0.02	1	0.730	4.248	4.460	0.00	0.418	4.421	4.421	7.97
15	S	0.02	2	0.730	4.248	4.461	0.00	0.409	4.417	4.421	8.10
15	S	0.04	1	0.710	4.240	4.428	0.00	0.410	4.404	4.377	7.69
15	L	0.02	1	0.730	4.248	4.460	0.00	0.406	4.417	4.419	7.80
20	S	0.02	1	0.730	4.600	4.504	0.00	0.415	4.762	4.453	5.39
20	S	0.02	2	0.730	4.600	4.505	0.00	0.415	4.762	4.458	5.39
20	S	0.04	1	0.710	4.598	4.467	0.00	0.414	4.754	4.401	5.12
20	L	0.02	1	0.730	4.600	4.504	0.00	0.406	4.768	4.450	5.44
30	S	0.02	1	0.730	5.044	4.546	0.00	0.409	5.210	4.458	3.54
30	S	0.02	2	0.730	5.044	4.553	0.00	0.400	5.206	4.480	3.68
30	S	0.04	1	0.710	5.046	4.497	0.00	0.417	5.190	4.392	3.30
30	L	0.02	1	0.730	5.044	4.546	0.00	0.417	5.190	4.473	3.39
35	L	0.02	1	0.730	5.198	4.555	0.00	0.419	5.338	4.470	2.99
60	S	0.02	1	0.730	5.688	4.556	0.00	0.403	5.823	4.397	2.24
60	S	0.02	2	0.730	5.688	4.588	0.00	0.403	5.823	4.457	2.24
60	S	0.04	1	0.710	5.691	4.466	0.00	0.401	5.818	4.238	2.12
60	L	0.02	1	0.730	5.688	4.556	0.00	0.411	5.810	4.411	2.13

Model 3 X_c	Model 3 $\log (L/L_\odot)$	Model 3 $\log T_e$	Model 3 $\tau(10^6$ yr)	Model 4 X_c	Model 4 $\log (L/L_\odot)$	Model 4 $\log T_e$	Model 4 $\tau(10^6$ yr)	Model 5 X_c	Model 5 $\log (L/L_\odot)$	Model 5 $\log T_e$	Model 5 $\tau(10^6$ yr)
0.212	3.417	4.245	37.30	0.041	3.468	4.216	42.67	0.0	3.521	4.253	43.64
0.208	3.365	4.207	41.94	0.030	3.421	4.171	47.86	0.0	3.479	4.206	48.71
0.212	3.956	4.311	19.28	0.039	4.015	4.269	22.15	0.0	4.071	4.310	22.67
0.203	3.931	4.267	20.76	0.030	3.997	4.206	23.80	0.0	4.054	4.248	24.22
0.200	4.519	4.359	10.95	0.019	4.592	4.277	12.58	0.0	4.639	4.324	12.71
0.206	4.506	4.367	10.99	0.018	4.583	4.289	12.77	0.0	4.633	4.340	12.90
0.201	4.502	4.300	10.83	0.012	4.582	4.174	12.63	0.0	4.636	4.228	12.71
0.208	4.503	4.365	10.48	0.021	4.578	4.286	12.20	0.0	4.628	4.333	12.35
0.214	4.848	4.383	7.41	0.013	4.925	4.272	8.84	0.0	4.973	4.324	8.90
0.214	4.848	4.392	7.40	0.018	4.925	4.277	8.78	0.0	4.974	4.336	8.88
0.204	4.848	4.292	7.28	0.013	4.920	4.024	8.60	0.0	4.977	4.129	8.68
0.201	4.855	4.375	7.47	0.016	4.930	4.253	8.71	0.0	4.977	4.306	8.80
0.213	5.300	4.329	4.97	0.040	5.351	4.007	5.81	...	...	...	...
0.208	5.294	4.368	5.14	0.036	5.353	4.008	6.05	...	...	...	...
0.204	5.286	4.197	4.92	0.134	5.307	3.946	5.32	...	...	...	...
0.200	5.272	4.363	4.81	0.011	5.336	4.123	5.68	0.0	5.379	4.237	5.73
0.212	5.414	4.350	4.23	0.039	5.464	4.008	4.99	...	...	...	...
0.208	5.884	4.039	3.10	...	...	...	...	...	...	...	...
0.209	5.884	4.014	3.10	...	...	...	...	...	...	...	...
0.321	5.842	3.994	2.51	...	...	...	...	...	...	...	...
0.188	5.874	4.076	3.09	...	...	...	...	...	...	...	...

is displayed in Figures 1, 2, 3, and 4. The evolutionary tracks for masses of 7, 10, 15, 30, and 60 $M_\odot$ are shown in Figure 5.

For masses greater than $\sim 10\ M_\odot$, the main new feature of Carson's opacities becomes important. This is a "bump" in the opacity curve due to the ultimate ionization of the CNO elements. It produces a local convective instability in the outer part of the envelope of the star. Since convection in such a region is non-adiabatic, the adopted choice of α_P affects to some extent the radius of the star, even though the mass of the outer convection zone does not exceed 10^{-3} of the total mass in any of the unevolved models. As evolution proceeds away from the ZAMS, the convection zone covers an increasingly large fraction of the star because the CNO "bump" in the opacity curve increases with decreasing density and because the mean temperature of the CNO ionization zone is associated with deeper layers of the star if the surface temperature is lower. Eventually, the separate convection zones due to hydrogen, helium, and CNO ionization merge completely into one large convection zone when the star attains a red-supergiant configuration.

On the other hand, the new atomic opacities have only a minor influence on the evolution of the deep interior of the star, where electron scattering dominates the opacity. Since the stellar luminosity is slightly reduced by the large size of the envelope opacities,

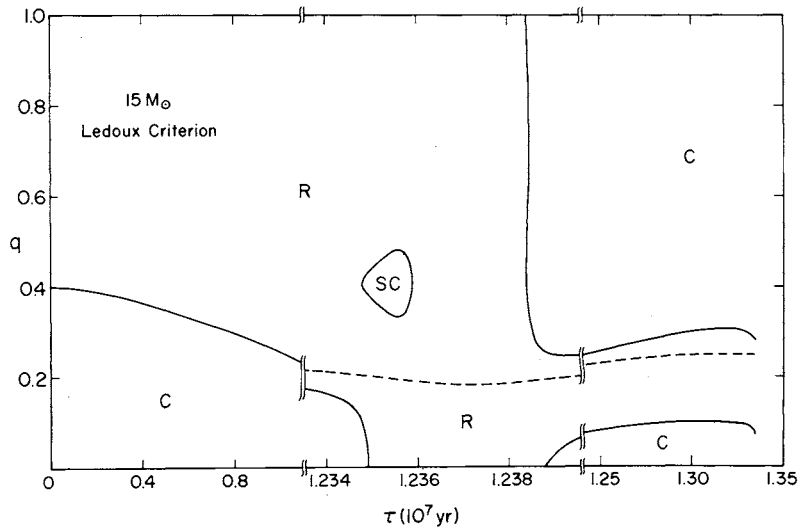

FIG. 1.—Evolution of the structural zones of a star of 15 $M_\odot$ with $(X_e, Z_e) = (0.73, 0.02)$. The Ledoux criterion for convection has been adopted. Coding is as follows: R, radiative; C, convective; SC, semiconvective. The dashed line represents the peak of the hydrogen-burning shell. The ordinate is mass fraction q. The abscissa, time, is divided into three segments, representing approximately the following three phases of evolution: (1) core hydrogen burning, (2) transitional stages, and (3) core helium burning.

convective instability in the layers which contain a gradient of mean molecular weight is marginally less than prevails in stellar models constructed with the earlier opacities. In these layers the convective instability appears temporarily as semiconvection shortly after the ZAMS stage for masses higher than $\sim 14\ M_\odot$ (Schwarzschild criterion) or $\sim 20\ M_\odot$ (Ledoux criterion), and also appears later, just before the instant of central hydrogen exhaustion, for masses higher than $\sim 6\ M_\odot$ (Schwarzschild criterion) or $\sim 8\ M_\odot$ (Ledoux criterion). When the Schwarzschild criterion is adopted for stars of high mass, full convection usually breaks out at the base of the semiconvective zone not long after the instant of central hydrogen exhaustion. However, in the new stellar models for masses greater than $\sim 30\ M_\odot$ $(Z_e = 0.02)$ or $\sim 20\ M_\odot$ $(Z_e = 0.04)$, convective instability in this part of the star is suppressed, first, by the sudden drop in luminosity as energy is taken out of the radiation field in the process of expanding the envelope to very large radii, and, later, by the cooling effect induced by the deep penetration of the surface convection zone into layers that would otherwise have been semiconvective.

Such a pronounced envelope expansion during the

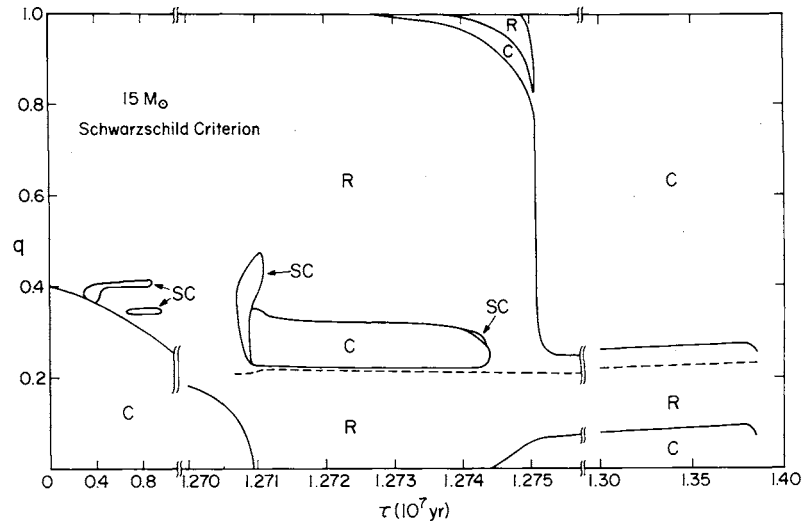

FIG. 2.—Evolution of the structural zones of a star of 15 $M_\odot$ with $(X_e, Z_e) = (0.73, 0.02)$. The Schwarzschild criterion for convection has been adopted. Coding is the same as in Fig. 1.

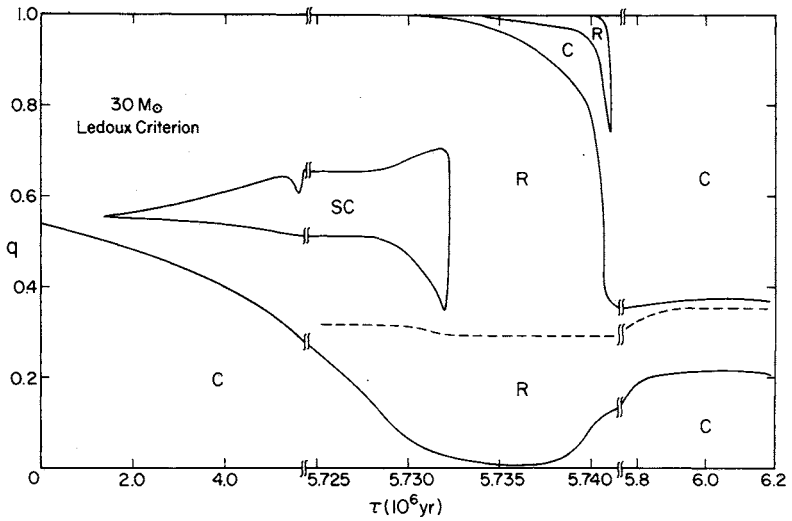

FIG. 3.—Evolution of the structural zones of a star of 30 $M_\odot$ with $(X_e, Z_e) = (0.73, 0.02)$. The Ledoux criterion for convection has been adopted. Coding is the same as in Fig. 1.

main phase of hydrogen burning occurs only at very high stellar masses. As a result, the star becomes successively a blue supergiant ($\log T_e > 4.0$), a yellow supergiant ($\log T_e = 4.0$–3.6), and a red supergiant ($\log T_e < 3.6$). The transition through the yellow-supergiant stages is very fast, occurring on the Kelvin time scale of the envelope. Effective temperatures drop at a rapid rate of ~ 0.1 K yr^{-1} (Schwarzschild criterion) or ~ 1 K yr^{-1} (Ledoux criterion). Very little hydrogen in the core is depleted at that time.

Past experience with models of massive stars in considerably later stages of evolution has shown that the yellow-supergiant region of the H-R diagram is characteristically avoided by thermally stable models, and that at least three static models for an advanced stage of evolution can usually be constructed with the same total mass and the same run of chemical composition. The three possible models characteristically turn out to be, respectively, a blue, a yellow, and a red supergiant, with the yellow-supergiant model being secularly unstable (e.g., Lauterborn and Siquig 1974; Gabriel, Refsdal, and Ritter 1974). Even for *unevolved* stellar models of very high mass constructed with Carson's opacities, static solutions exhibit the same type of multiplicity over a limited mass range, though the three models span a much narrower range of effective temperature than do the supergiant models (Stothers 1974*b*). Therefore, it is of interest to deter-

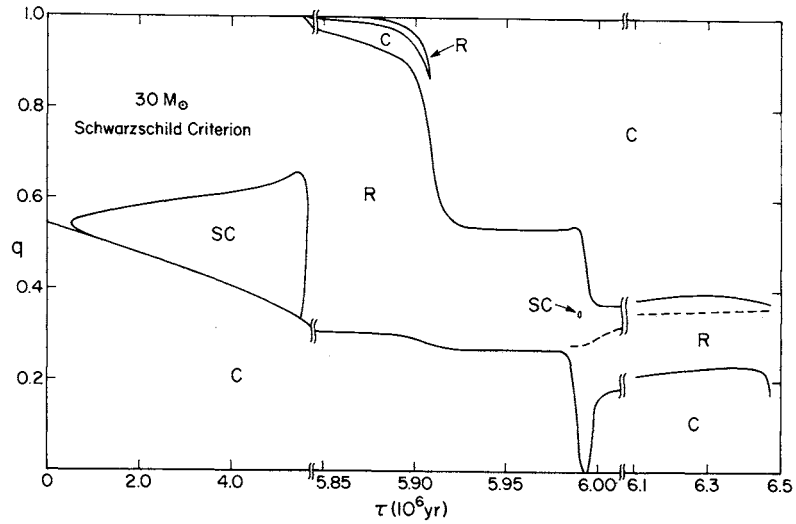

FIG. 4.—Evolution of the structural zones of a star of 30 $M_\odot$ with $(X_e, Z_e) = (0.73, 0.02)$. The Schwarzschild criterion for convection has been adopted. Coding is the same as in Fig. 1.

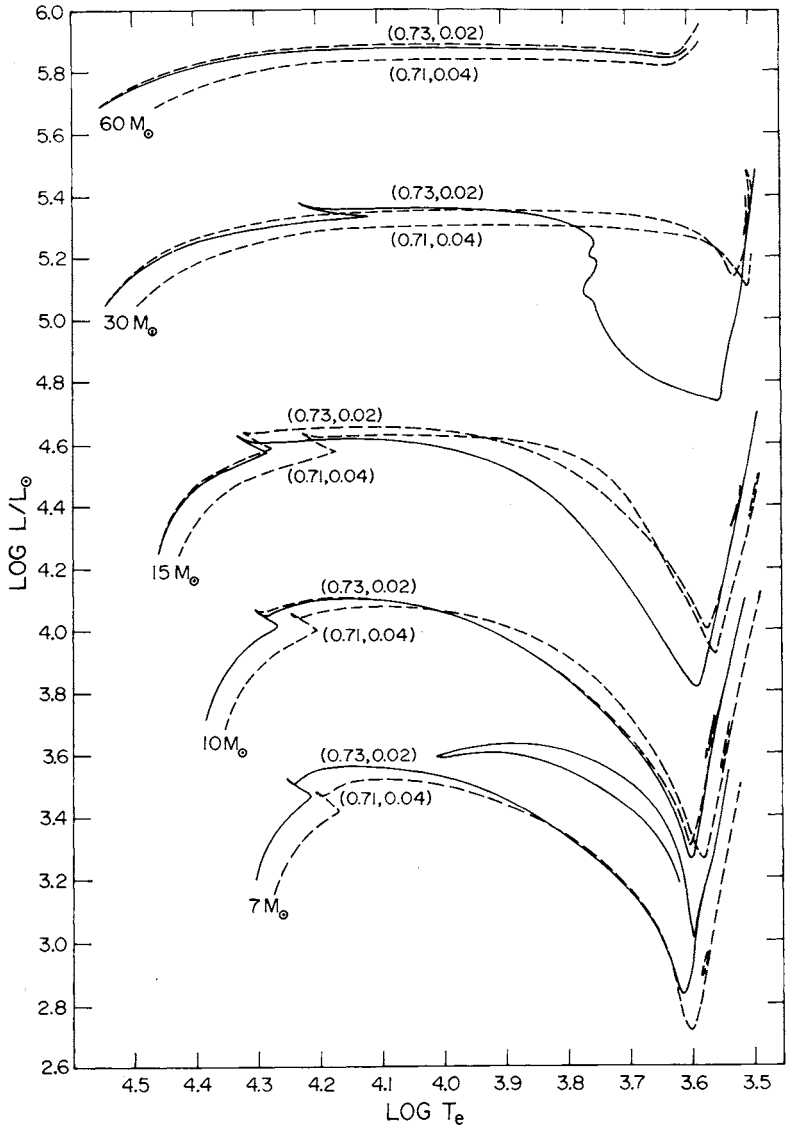

FIG. 5.—Theoretical evolutionary tracks in the H-R diagram for stars of 7, 10, 15, 30, and 60 $M_\odot$. Tracks are labeled with (X_e, Z_e). The criterion for convection is either the Ledoux criterion (*continuous lines*) or the Schwarzschild criterion (*dashed lines*).

mine whether multiple solutions exist also for the present partially evolved models.

We have selected as a test case 60 $M_\odot$ and have looked for static blue-supergiant and yellow-supergiant models at several stages of evolution. (Unfortunately, technical problems have prevented us from looking for static red-supergiant models.) It turns out that a decrease in the central hydrogen abundance has the same effect on the present models as does an increase of the total stellar mass for the unevolved models of extremely high mass. For a large central hydrogen abundance, only one model—a blue supergiant—exists. As the central hydrogen abundance is lowered, the effective temperature of the model decreases. At a certain stage, a second model—a yellow supergiant—also appears, although it is probably secularly unstable. With a further decrease of the central hydrogen abundance, the blue and yellow models approach each other in effective temperature until they finally merge (at approximately $\log T_e = 4.0$). After this critical stage, no static blue-supergiant or yellow-supergiant model exists at all.

On the basis of our detailed evolutionary sequences, we find it probable that no *secularly stable*, static red-supergiant model exists either, at least above a certain mass, which is probably greater than 30 $M_\odot$ ($Z_e = 0.02$) or 20 $M_\odot$ ($Z_e = 0.04$). For masses higher than this, it has not been possible to calculate the evolutionary tracks much past the yellow-supergiant phase because of the increasingly violent thermal oscillations of the outer envelope, which have a time scale approaching the dynamical (pulsational) time

scale. (In Fig. 5 a few thermal oscillations show up in the yellow-supergiant region for 30 $M_\odot$ with Z_e = 0.02, because the star is already highly centrally condensed well before reaching the red-supergiant region.) This dramatic behavior may possibly be explained by the results of our earlier study of unevolved models, in which only one solution was found to exist at any mass lying above the narrow mass range of multiple models, and this solution, for a sufficiently high stellar mass, was secularly unstable. We speculate that the stellar envelope may be shed as a result of the increasingly violent instability.

b) Core Helium Burning

In the new evolutionary sequences that were carried beyond the end of core hydrogen burning, the top of the red-supergiant branch in the H-R diagram is always attained shortly after core helium ignition, when only 1% of the helium in the core has been consumed. The surface hydrogen abundance is reduced at that time by 3–14% as a result of mixing due to the penetration of the outer convective envelope into the helium-rich layers, the reduction being greatest for the highest stellar masses and for the largest initial metals abundances.

It is a remarkable fact that the large size of the new envelope opacities overwhelms all opposing factors that might tend to collapse the star back into a blue-supergiant configuration (see Papers III and IV). Of course, it is possible that a more sophisticated treatment of convection in the outer envelope would lead to the development of a "blue loop" on the H-R diagram, but we have at present no way of evaluating this possibility except by varying α_P (which is found to lead to no changes). On the other hand, a high density or a low metals abundance induces a small CNO opacity. Therefore, it is only those stellar models with the smallest masses and the smallest initial metals abundances that are found to be capable of collapsing during core helium burning into the blue-supergiant configuration. The critical stellar mass for this to happen is $\sim 10\ M_\odot$, $\sim 8\ M_\odot$, and (probably) $\sim 6\ M_\odot$, for an initial metals abundance of Z_e = 0.01, 0.02, and 0.04, respectively. These masses are only weakly dependent on X_e, α_P, and the specified criterion for convection. All the sequences actually calculated are listed in Table 2.

An additional sequence for 7 $M_\odot$ has been computed with (X_e, Z_e) = (0.73, 0.02) and with the convective mixing length taken to be equal to 0.4 times the *density* scale height (Carson and Stothers 1976). This sequence seems to agree well with the present sequence for 7 $M_\odot$ (with the minor exception of a reversal of the relative luminosities of the second and third crossings of the Hertzsprung gap). Most of the present sequences for the mass range 7–15 $M_\odot$ are reminiscent of those sequences based on the Cox-Stewart opacities that have large initial hydrogen and metals abundances (i.e., in which the envelope opacities are high).

III. COMPARISON WITH OBSERVATIONS

The Carson and Cox-Stewart opacities make very different predictions for the location of stars of high mass in the H-R diagram, especially if the stellar mass exceeds $\sim 15\ M_\odot$. In the case of the Cox-Stewart opacities, the main-sequence band of stars burning core hydrogen is everywhere a very narrow zone, as depicted in many papers (e.g., Fig. 7 of Paper IV).

TABLE 2

NEW EVOLUTIONARY SEQUENCES OF MODELS FOR STARS OF 7, 10, 15, 20, AND 30 $M_\odot$ THROUGH CORE HELIUM EXHAUSTION*

$M/M_\odot$	Criterion for Convection	X_e	Z_e	α_P	log T_e (tip)	log T_e (b/y)	τ_H (10^6 yr)	τ_{He}/τ_H	τ_b/τ_{He} (loop)
7.....	S or L	0.73	0.02	1	4.01	~3.9	43.691	0.156	0.402
7.....	S or L	0.71	0.04	1	...	...	48.771	0.163	...
10.....	S	0.74	0.01	1	4.17	~4.0	22.438	0.139	0.598
10.....	S	0.73	0.02	1	...	...	22.674	0.126	...
10.....	S	0.73	0.02	2	...	...	22.674	0.129	...
10.....	S	0.71	0.04	1	...	...	24.221	0.121	...
10.....	S	0.67	0.02	1	...	...	17.788	0.155	...
10.....	L	0.74	0.01	1	(†)	(†)	22.456	0.119	(†)
10.....	L	0.73	0.02	1	...	...	22.670	0.119	...
10.....	L	0.73	0.02	2	...	...	22.670	0.115	...
10.....	L	0.71	0.04	1	...	...	24.238	0.112	...
10.....	L	0.67	0.02	1	...	...	17.779	0.129	...
15.....	S	0.74	0.01	1	...	...	12.792	0.102	...
15.....	S	0.73	0.02	1	...	...	12.709	0.101	...
15.....	S	0.71	0.04	1	...	...	12.704	0.101	...
15.....	L	0.74	0.01	1	...	...	12.493	0.088	...
15.....	L	0.73	0.02	1	...	...	12.349	0.089	...
20.....	S	0.71	0.04	1	...	...	8.681	0.087	...
30.....	S	0.73	0.02	1	...	...	5.987	0.079	...
30.....	L	0.73	0.02	1	...	...	5.727	0.083	...

* $\theta_{\alpha}{}^2 = 0.1$ and "new" $\epsilon_{3\alpha}$. Notation follows that of Papers III and IV.

† This sequence almost developed a blue loop when $Y_c \approx 0.4$.

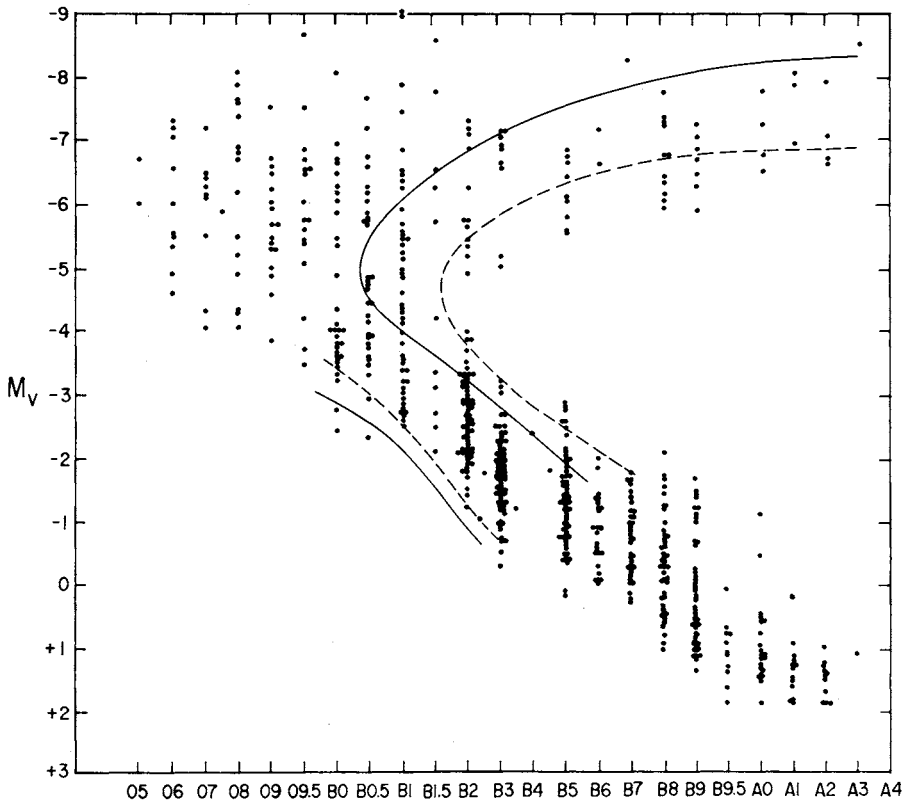

FIG. 6.—Theoretical main-sequence bands for the new stellar models burning core hydrogen are superposed on an observational H-R diagram for bright early-type stars, taken from the work of Andrews. The assumed initial metals abundances are $Z_e = 0.02$ (*continuous lines*) and $Z_e = 0.04$ (*dashed lines*). The comparison with O stars is not shown (see text).

But in the case of Carson's opacities the band of stars flares out toward cool effective temperatures as the luminosity rises beyond $\log (L/L_\odot) = 4.5$.

The left-hand boundary of the zone, representing the ZAMS line, has already been compared with observations (Stothers 1976). However, no clear choice between the Carson and Cox-Stewart opacities could be made because the effective temperatures of O stars are too uncertain. We shall here consider primarily the right-hand boundary, which avoids the use of O stars. In Figure 6 are plotted the most extensive available *homogeneous* data for stars of early spectral type (Andrews 1968). All the luminosities have been determined from measurements of the equivalent width of Hα, with the calibration based on a substantial number of stars in clusters with accurately determined distances. The theoretical lines representing the hot and cool edges of the predicted main-sequence band for Carson's opacities have been converted to observational coordinates by using Johnson's (1966) relations. Three empirical features of Figure 6 ought to be noticed: (1) the unbroken distribution of O5–B1 stars; (2) the sudden bifurcation of the stellar distribution into "dwarf" and "supergiant" branches beginning at (M_V, Sp) = (−4.5, B1); and (3) the concentration of the *bolometrically* brightest stars toward very early spectral types. These features are explained surprisingly well by the new stellar models burning core hydrogen, particularly if the initial metals abundance is high, e.g., if $Z_e = 0.04$ (or, alternatively, α_P could be reduced to a value less than unity).

In order to analyze the cooler part of the H-R diagram not covered in Figure 6, it is necessary to resort to stars in clusters and associations with known distances. Since accurate luminosities are important here, we shall not use the composite H-R diagram of Humphreys (1970), in which the luminosities of many of the fainter stars are unreliable because their group membership is uncertain. Rather, we shall use only the most certain members of clusters and associations selected from the two lists of Stothers (1969, 1972) with the help of more recently published membership criteria for some of the stars; the stars from the cluster NGC 2439 (White 1975) will also be used. In Figure 7 are plotted the final selection of stars of luminosity class I, whose probable masses range upward from $\sim 10\ M_\odot$.

The theoretically predicted "gap" covering spectral types A, F, G, and K agrees very well with the gap actually observed. Since the location of the gap is predicted to be independent of luminosity, Humphrey's (1970) more numerous data have also been consulted to confirm that this is indeed the case. At spectral type M the observed clumping of supergiants

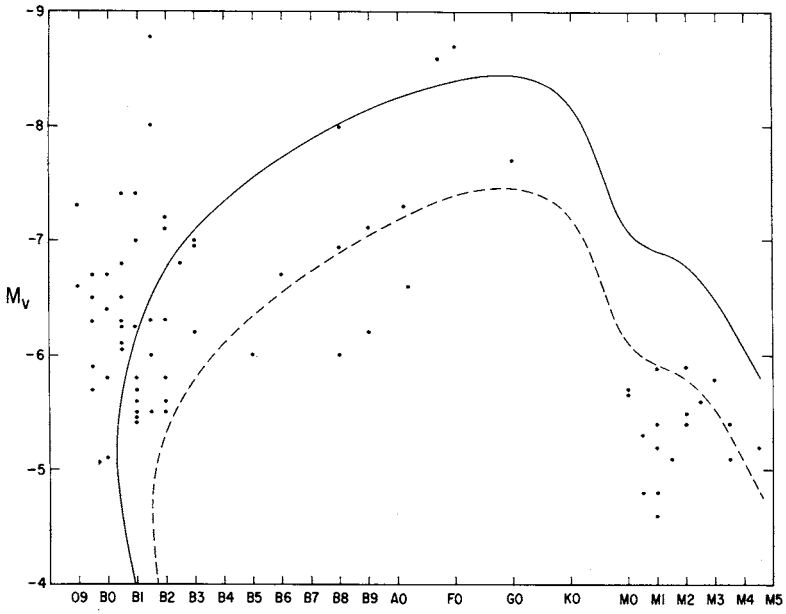

FIG. 7.—Cool edges of the theoretical main-sequence bands for the new stellar models burning core hydrogen are superposed on an observational H-R diagram for luminous supergiants that are members of clusters and associations. The assumed initial metals abundances are $Z_e = 0.02$ (*continuous line*) and $Z_e = 0.04$ (*dashed line*). Stars lying above these lines are interpreted as mostly burning core hydrogen.

is adequately explained by stellar models burning core helium (and, possibly, heavier elements); a few of the very brightest M supergiants may still be burning core hydrogen. Finally, the greater luminosity of early-type supergiants compared with M supergiants in the same star cluster (Stothers 1969) can be satisfactorily explained by the faintness of the new models for core helium burning, as Table 3 indicates.

According to the interpretation given here, the upper main sequence on the H-R diagram branches out like a rainbow arc over all spectral types at the brightest luminosities. But two difficulties with this picture arise. The first difficulty is the appearance of a scattering of B5–A2 supergiants with relatively low luminosities in Figures 6 and 7. Unless the true opacity (or Z_e) is larger than expected or observational errors are at fault, these stars are unexplained by the new evolutionary tracks for the phase of core hydrogen burning. Moreover, unless Z_e is *smaller* than expected, a "blue loop" does not occur during core helium burning for masses greater than $\sim 7\ M_\odot$ ($M_V < -4$). The second difficulty is the striking absence of M supergiants more massive than $\sim 25\ M_\odot$ (this difficulty is also encountered by models constructed with the Cox-Stewart opacities). A possible resolution of these two difficulties is that mass loss, at a rate increasing with stellar luminosity, removes stars from the region of M supergiants. (Neutrino emission cannot accomplish this because the neutrino loss rates are negligible during core hydrogen and helium burning.) In fact, there is evidence for evolution from M to earlier spectral types from the presence of dust shells around some yellow supergiants (Stothers 1975). Therefore, the domain of early-type supergiants could be populated by stars in all phases of evolution, from pre–main-sequence to pre-supernova. Only an accurate determination of surface gravity and radius would permit one to ascertain whether a particular supergiant has a normal or a deficient mass.

The difficulties found in the case of the present stellar models seem rather minor in comparison with the more fundamental difficulties encountered by the use of the Cox-Stewart opacities (see Paper IV and Stothers 1976). Therefore, the next step to take might be a recalculation of the evolutionary sequences based on Carson's opacities with an allowance for substantial mass loss.

TABLE 3

THEORETICALLY PREDICTED LUMINOSITIES FOR SUPERGIANTS WITH $Z_e = 0.04$ BURNING CORE HELIUM

$M/M_\odot$	$\log (L/L_\odot)$ (blue)	$\log (L/L_\odot)$ (red)	ΔM_{bol}
7	3.5	3.0	1.2
10	4.0	3.6	1.0
15	4.6	4.4	0.5
20	5.0	4.8	0.5

We thank T. Richard Carson for permission to use his new radiative opacities in advance of their publication. Inquiries concerning these opacities may be addressed to Dr. Carson at the University Observatory, St. Andrews, Scotland.

REFERENCES

Andrews, P. J. 1968, *Mem. R.A.S.*, **72**, 35.
Carson, T. R. 1976, in preparation.
Carson, T. R., and Stothers, R. 1976, *Ap. J.*, **204**, 461.
Gabriel, M., Refsdal, S., and Ritter, H. 1974, *Astr. Ap.*, **32**, 217.
Humphreys, R. M. 1970, *Ap. Letters*, **6**, 1.
Johnson, H. L. 1966, *Ann. Rev. Astr. Ap.*, **4**, 193.
Lauterborn, D., and Siquig, R. 1974, *Astr. Ap.*, **30**, 385.
Stothers, R. 1969, *Ap. J.*, **155**, 935.
Stothers, R. 1972, *Ap. J.*, **175**, 717.
———. 1974*a*, *Ap. J.*, **194**, 651.
———. 1974*b*, *Ap. J.*, **194**, 699.
———. 1975, *Ap. J.* (*Letters*), **197**, L25.
———. 1976, *Ap. J.*, **209**, 800.
Stothers, R., and Chin, C.-w. 1975, *Ap. J.*, **198**, 407 (Paper III).
———. 1976, *Ap. J.*, **204**, 472 (Paper IV).
White, S. D. M. 1975, *Ap. J.*, **197**, 67.

CHAO-WEN CHIN and RICHARD STOTHERS: Institute for Space Studies, Goddard Space Flight Center, NASA, 2880 Broadway, New York, NY 10025